

Multiwavelength characterization of two flaring blazars: insight into the emission region of intermediate-synchrotron-peaked BL Lacs

S. Loporchio,^{a,*} G. Bonnoli,^b D. Cerasole,^a L. Di Venere,^a D. Dominis Prester,^c F. Giordano,^a E. Lindfors,^d M. Manganaro^c and L. Pavletić^c on behalf of the *Fermi*-LAT and MAGIC Collaborations[†]

^a*INFN MAGIC Group: INFN Sezione di Bari and Dipartimento Interateneo di Fisica dell'Università e del Politecnico di Bari, I-70125 Bari, Italy*

^b*National Institute for Astrophysics (INAF), I-00136 Rome, Italy*

^c*Croatian MAGIC Group: University of Rijeka, Faculty of Physics, 51000 Rijeka, Croatia*

^d*Finnish MAGIC Group: Finnish Centre for Astronomy with ESO, University of Turku, FI-20014 Turku, Finland*

E-mail: serena.loporchio@ba.infn.it

The blazars B2 1811+31 and GB6 J1058+2817 were found to be in flaring state during 2020 and 2021, respectively. The high states of the sources were registered by the *Fermi*-LAT at energies below 100 GeV, triggering observations at higher energies with the MAGIC telescopes, in the UV/X rays with the *Swift* satellite and with ground-based radio and optical telescopes. The observations in the very-high-energy (VHE, 100 GeV < E < 100 TeV) gamma-ray band led to the first detection of both sources in this energy range. A long-term gamma-ray lightcurve was derived using *Fermi*-LAT data, identifying the time intervals in which the two sources persisted in a quiet state. Archival data collected in the radio to X-ray wavelengths showed that the two sources exhibited intermediate-synchrotron-peaked BL Lac behaviors in their low states, rather rare sources in the TeV sky. The high state of the two sources was deeply investigated thanks to the coverage provided by multi-wavelength (MWL) observational campaigns. In this contribution, we present the results of the gamma-ray observations which are included in a MWL observational campaign organized on these sources during their high-states. We discuss the flare spectral properties and temporal variability. In the high-energy gamma band, sub-daily-scale variability and strong spectral hardening give evidence for compact emission regions responsible for the radiative output at high energies during the flare.

38th International Cosmic Ray Conference (ICRC2023)
26 July - 3 August, 2023
Nagoya, Japan



*Speaker

[†]a complete list of the MAGIC Collaboration authors can be found at the end of the proceedings

1. Introduction

Blazars are jetted active galactic nuclei (AGNs) with their relativistic jets of plasma streams pointed toward the observer. They are the most numerous gamma-ray sources in the extragalactic sky. The spectral energy distribution (SED) of blazars exhibits a two bump non-thermal continuum produced within the jet and boosted by relativistic effects, ranging from radio to gamma-ray energies [1]. The first bump in the SED, peaking in the frequency range from infrared to X-rays, is usually interpreted as synchrotron emission from ultra-relativistic electrons accelerated within the jet, while the high-energy (HE) bump peaks above MeV energies and it is commonly attributed to inverse Compton (IC) scattering of low-energy photons. The seed photons for the IC scattering can be produced within the jet via synchrotron radiation (synchrotron self-Compton, SSC) but they can also originate externally to the jet; the latter case is often referred to as external Compton (EC).

Blazars can be further divided into two sub-classes [2]: flat spectrum radio quasars (FSRQs) and BL Lac objects (BL Lacs) depending on the presence of emission or absorption lines associated with the emission of the broad and narrow line region in addition to a thermal component associated with the accretion disk. Both blazar classes show rapidly variable luminosity in all wavelengths, strong polarization in the optical range and emission up to gamma-ray energies.

The peak frequency of the synchrotron bump ν_{synch} in the SED leads to a further classification of BL Lacs into low-, intermediate-, and high-frequency peaked sources (LBL, $\nu_{\text{synch}} < 10^{14}$ Hz, IBL, $10^{14} \text{ Hz} < \nu_{\text{synch}} < 10^{15}$ Hz and HBL, $\nu_{\text{synch}} > 10^{15}$ Hz, respectively [3]), with most of the TeV emitting BL Lacs being classified as HBL, while the location of the first peak is usually at quite low frequencies for FSRQs. A good coverage in the energy range from optical to X-rays is essential to properly estimate the peak frequency and classify the source. Only a complete energy coverage from the radio to TeV energy range (multi-wavelength observations, MWL) allows for a proper understanding of the emission mechanisms in order to extrapolate the basic physical quantities of the emission region, for example the size of the emission region, the Doppler factor and the magnetic field intensity. Moreover, given the variability of the objects, shown in different energy ranges, simultaneous observations are required. However, especially for weak and distant blazars, a complete coverage may be difficult to obtain. While the HBL class has been largely studied at very-high-energy (VHE, ≥ 100 GeV) gamma-rays thanks to Imaging Air Cherenkov Telescopes (IACTs) observations, few IBL and LBL are detected up to TeV energies.

Up to and including the *Fermi*-LAT Fourth Source Catalog [4], the blazars B2 1811+31 (redshift $z=0.117$ [5]) and GB6 J1058+2817 (its redshift is not well established, with a tentative value of $z=0.4793$ [6]) are classified as BL Lac objects, respectively as an IBL, following [7], and as a BL Lac of unclear class. Recently, triggered by the enhanced high-energy gamma-ray activity reported by the *Fermi*-LAT during October 2020 [8] and March 2021 [9], MWL observational data on these two under-examined sources were collected. The observations in the VHE regime performed by the MAGIC telescopes led to the first detection of both sources in this energy range [11, 12]. Moreover, simultaneous or quasi-simultaneous observations were performed by several optical and radio telescopes. In this contribution, we will report on the observations performed by the MAGIC telescopes and by the *Fermi*-LAT satellite. These observations are part of a wider MWL campaign which involves data from radio to VHE, with studies on the long- and short-term multi-band variability and broadband modeling of the SED. The details of this study will be reported

in a paper (in prep).

2. Very-high-energy gamma-ray observations

MAGIC is a stereoscopic system of two 17 m diameter imaging Cherenkov telescopes located at an altitude of 2200 m in the Roque de los Muchachos Observatory [10]. The MAGIC telescopes performed observations of the two sources shortly after the triggers reported by *Fermi*-LAT. The analysis of the data was performed with the standard tool for the MAGIC analysis, MARS [13].

After the *Fermi*-LAT trigger, MAGIC telescopes observes the source B2 1811+31 starting from MJD 59127 (October 5, 2020) to MJD 59133 (October 11, 2020) in dark conditions and wide zenith angle range, from 20° to 65° , while the source GB6 J1058+2817 was observed from MJD 59306 (April 2, 2021) to MJD 59309 (April 5, 2021) at low zenith distance, from 5° to 35° , also in dark conditions.

The standard variable θ^2 , which is defined as the squared angular distance of the reconstructed shower direction with respect to the source location in the camera, was used to look for any significant VHE gamma-ray excess with respect to background. The observations carried out during the flaring period led to a significant detection in the VHE range with a statistical significance of 5.3σ for B2 1811+31 and 6.0σ for GB6 J1058+2817. The statistical significance is estimated using the Li&Ma formula reported in [14].

We then derived the night-wise gamma-ray flux for energies above 135 GeV and 100 GeV for B2 1811+31 and GB6 J1058+2817, respectively. The energy threshold was employed to allow for a proper flux estimation for each night while still taking into account the observational conditions. The resulting light curves are shown in Figure 1, where 95% confidence upper limits are indicated as downward arrows in VHE gamma rays when the flux is compatible with zero. The light curves show no significant variability in the VHE range. We also looked for intra-night variability, but due to lack of statistics we could not investigate it further.

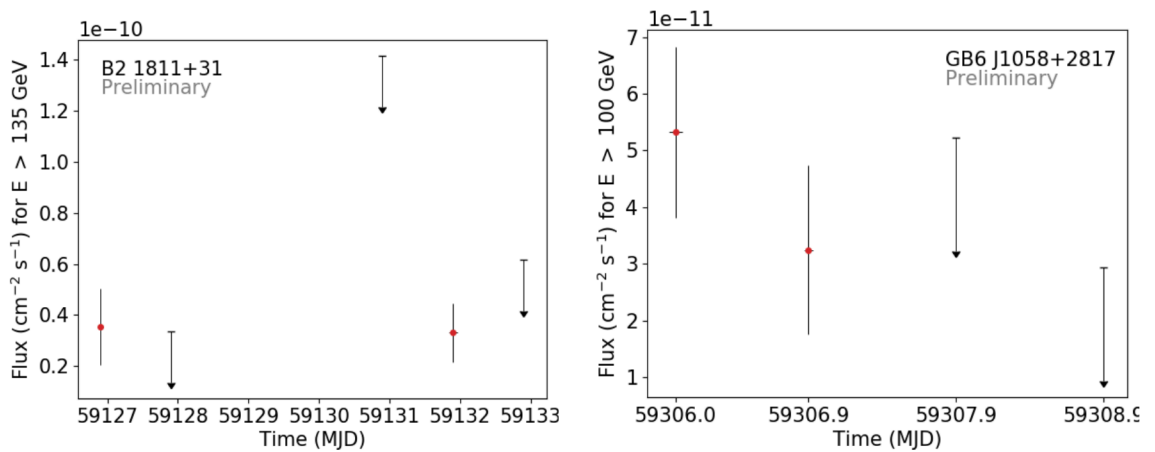


Figure 1: Night-wise light curves in the VHE gamma-ray energy range for the two sources: B2 1811+31 (left) and GB6 J1058+2817 (right). 95% confidence upper limits are indicated as downward arrows in VHE gamma rays when the flux is compatible with zero.

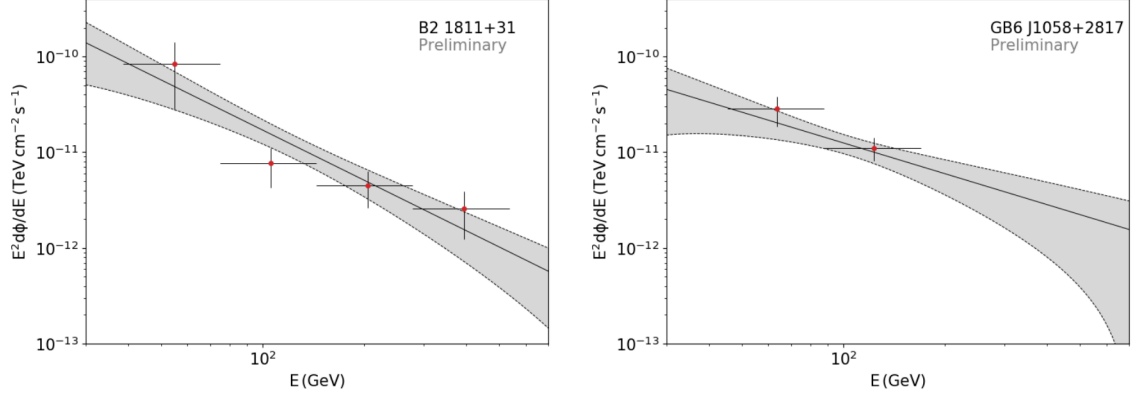


Figure 2: Differential energy spectrum of B2 1811+31 (left) and GB6 J1058+2817 (right) measured by MAGIC and corrected for EBL (red circles). The black solid line represents the best-fit power-law, while the gray shaded area represents the systematic uncertainties of the analysis.

The data acquired during all the nights were combined to evaluate the overall spectrum, since the acquired signal was not strong enough to evaluate the spectrum for each night individually. The resulting spectrum was fitted with a power-law function. In order to reconstruct the intrinsic spectrum of the source, the observed spectrum was unfolded by the energy dispersion using the Bertero method [15] and then corrected for the extragalactic background light (EBL) absorption by adopting the Domínguez model [16]. For the EBL correction, we adopted $z=0.117$ for B2 1811+31 and $z=0.4793$ for GB6 J1058+2817.

The MAGIC spectrum obtained after the unfolding and the EBL correction is shown in Figure 2. As can be seen, the spectrum is soft and it is well-described by a simple power-law model for both sources:

$$\frac{dN}{dE} = N_0 \left(\frac{E}{E_0} \right)^{-\Gamma} \quad (1)$$

with photon index $\Gamma = 3.75 \pm 0.40_{\text{stat}}$, decorrelation energy $E_0 = 125.16 \text{ GeV}$ and normalization constant $N_0 = (7.36 \pm 1.99_{\text{stat}}) \times 10^{-10} \text{ TeV}^{-1} \cdot \text{cm}^{-2} \cdot \text{s}^{-1}$ for B2 1811+31, and $\Gamma = 3.39 \pm 0.32_{\text{stat}}$, $E_0 = 161.11 \text{ GeV}$ and $N_0 = (1.95 \pm 0.54_{\text{stat}}) \times 10^{-10} \text{ TeV}^{-1} \cdot \text{cm}^{-2} \cdot \text{s}^{-1}$ for GB6 J1058+2817. For both sources, the soft spectrum in the VHE range suggests that the high-energy bump in their SEDs is likely to be peaking at GeV energies.

3. *Fermi*-LAT data analysis

The Large Area Telescope (LAT) instrument onboard the *Fermi Gamma-Ray Space Telescope* satellite is a pair-conversion telescope with a precision converter-tracker and calorimeter that detects gamma rays from tens of MeV to 1 TeV [17].

Data from B2 1811+31 and GB6 J1058+2817 were selected since the start of the *Fermi* mission at first, and then in a reduced time window in temporal coincidence with the MAGIC observations. Events in a 15° region of interest (ROI) centered on the nominal position of the sources of interest and reconstructed energy in the 100 MeV – 1 TeV range were selected. The cuts on the quality and the zenith distance were chosen following the recommendations by the *Fermi*-LAT collaboration.

Standard cuts on the quality were used, e.g. 'DATA_QUAL>0 && LAT_CONFIG==1', while a zenith distance $< 90^\circ$ to reduce the contamination from the Earth limb was selected.

The analysis of *Fermi*-LAT data was performed using ScienceTools v2.0.8, fermipy v1.0.1¹ and the P8R3_SOURCE_V2 instrument response function. We performed a binned likelihood analysis in a square region inscribed in the ROI selected. All the localized sources included in the 4FGL [4] within 20° from the source were included in the model, along with the Galactic interstellar diffuse and residual background isotropic emission, as modeled respectively ingll_iem_v07 and iso_P8R3_SOURCE_V3_v1.txt². Data were binned in energy adopting 8 bins/decade. Spectral parameters of all the point-like sources in the ROI within 5° from the two sources of interest were left free to vary in the model. The spectra of the diffuse components, both galactic and isotropic, were also left free to vary. The parameters of all other sources were fixed to the published 4FGL values.

In order to investigate the high-energy gamma-ray variability of the two sources of interest, we produced light curves with equally-spaced time bins. A dedicated likelihood analysis in each temporal bin was performed. The bi-weekly light curves since 2008 for the two sources are represented in Figure 3. A general quiescent state can be seen, with the flux suddenly increasing in the flare periods, which lasts for about 250 days for B2 1811+31, and 40 days for GB6 J1058+2817, highlighted with a gray shaded area in Figure 3.

The spectral features of the two sources in the time intervals before, during and after the flare were analysed by performing dedicated fit. In the flare period, shown in Figure 4 the spectra of both sources are well described by a power-law model, with spectral index $\Gamma = 1.83 \pm 0.02$ for B2 1811+31 and $\Gamma = 1.81 \pm 0.04$, both hardening with respect to the periods before the flaring activity and then softening after the flaring activity stops.

4. Conclusions

We report here on part of a MWL analysis performed on the BL Lac objects B2 1811+31 and GB6 J1058+2817, both observed during flaring state with respect to previous observations. Both the examined sources exhibit a soft VHE spectrum, with spectra index ranging between 3 and 4 in this energy range. No variability in the VHE gamma-ray was found in the period under investigation. On the other hand, the observations in the *Fermi* range showed a quiescent state of both sources in the past, with a sudden increase in the HE gamma-ray activity in the flare periods. In these time intervals, both sources showed a spectral hardening in this energy range with respect to previous observations.

These sources were not studied in detail before these observations, with none to rare observations in the whole electromagnetic spectrum, and the redshift of GB6 J1058+2817 is not well established yet, as well as its classification among the different BL Lacs subclasses. Investigations of observations collected during or close to the flaring activity in lower energy ranges are currently ongoing, in particular in the optical/X-ray band, in order to study the synchrotron peak position and properly classify the sources. Studies on the possible variability of the sources are also ongoing, in order to constrain the size of the emission region, which will then be employed to model the SED of

¹<https://fermipy.readthedocs.io/en/latest/>

²<https://fermi.gsfc.nasa.gov/ssc/data/access/lat/BackgroundModels.html>

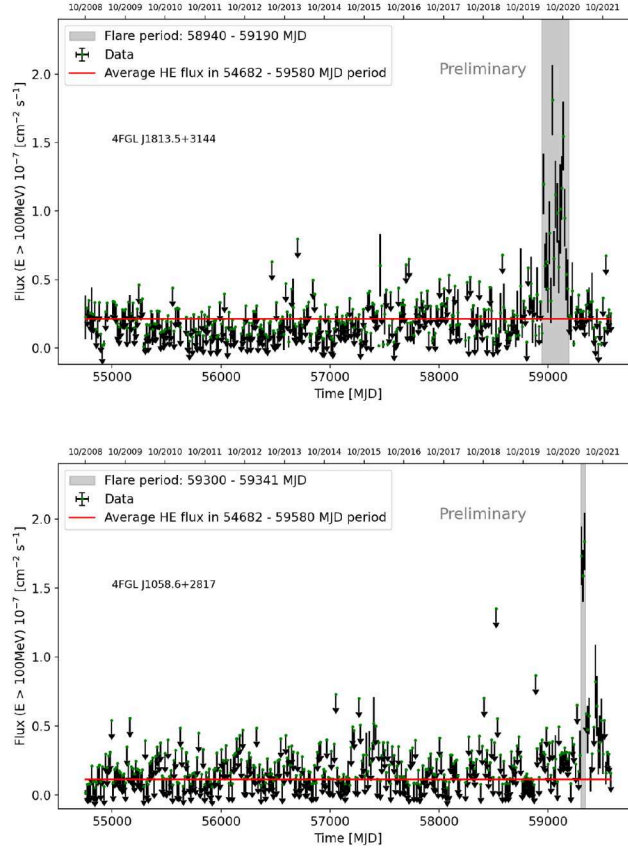


Figure 3: Gamma-ray flux light curves of B2 1811+31 (top) and GB6 J1058+2817 (bottom) measured with the *Fermi*-LAT since the beginning of the mission, bi-weekly binned. The gray shaded area marks the flare period. 95% C.L. upper limits are shown as downward arrows for each time bin where the TS value for the source was found to be smaller than 9. The average flux from the analyzed period is shown as a red solid line.

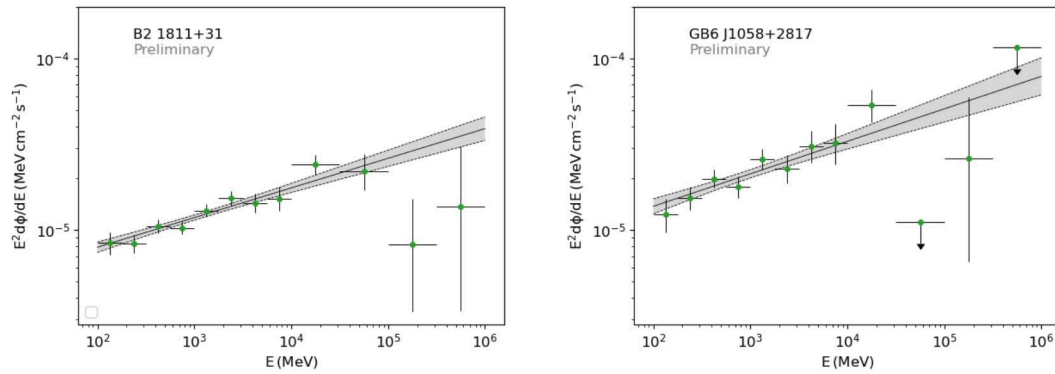


Figure 4: Differential energy spectrum of B2 1811+31 (left) and GB6 J1058+2817 (right) as measured by the *Fermi*-LAT in the flare period.

the sources, in order to investigate the emission mechanism of this little studies subclass of blazars, which fills the gap between LBLs and HBLs, playing an important role for BL Lac unification theories.

Acknowledgments

We would like to thank the Instituto de Astrofísica de Canarias for the excellent working conditions at the Observatorio del Roque de los Muchachos in La Palma. The financial support of the German BMBF, MPG and HGF; the Italian INFN and INAF; the Swiss National Fund SNF; the grants PID2019-104114RB-C31, PID2019-104114RB-C32, PID2019-104114RB-C33, PID2019-105510GB-C31, PID2019-107847RB-C41, PID2019-107847RB-C42, PID2019-107847RB-C44, PID2019-107988GB-C22 funded by MCIN/AEI/ 10.13039/501100011033; the Indian Department of Atomic Energy; the Japanese ICRR, the University of Tokyo, JSPS, and MEXT; the Bulgarian Ministry of Education and Science, National RI Roadmap Project DO1-400/18.12.2020 and the Academy of Finland grant nr. 320045 is gratefully acknowledged. This work was also been supported by Centros de Excelencia “Severo Ochoa” y Unidades “María de Maeztu” program of the MCIN/AEI/ 10.13039/501100011033 (SEV-2016-0588, SEV-2017-0709, CEX2019-000920-S, CEX2019-000918-M, MDM-2015-0509-18-2) and by the CERCA institution of the Generalitat de Catalunya; by the Croatian Science Foundation (HrZZ) Project IP-2016-06-9782 and the University of Rijeka Project uniri-prirod-18-48; by the Deutsche Forschungsgemeinschaft (SFB1491 and SFB876); the Polish Ministry Of Education and Science grant No. 2021/WK/08; and by the Brazilian MCTIC, CNPq and FAPERJ.

References

- [1] Urry, C. M. and Padovani, P. (1995). Unified Schemes for Radio-Loud Active Galactic Nuclei. Publications of the Astronomical Society of the Pacific, 107:803.
- [2] Landt H., Padovani, P., Perlman, E. S., and Giommi, P. (2004). A physical classification scheme for blazars. Monthly Notices of the Royal Astronomical Society, Volume 351, Issue 1, pp. 83-100.
- [3] A. A. Abdo et al. (2010). The Spectral Energy Distribution of Fermi Bright Blazars. The Astrophysical Journal, Volume 716, Issue 1, pp. 30-70.
- [4] Abdollahi, S. et al. (2020). Fermi Large Area Telescope Fourth Source Catalog. The Astrophysical Journal Supplement Series, Volume 247, Issue 1, id.33, 37 pp.
- [5] Giommi P., Tagliaferri G., Beuermann K., et al. (1991). The EXOSAT High Galactic Latitude Survey. The Astrophysical Journal, 378, 77.
- [6] Massaro F., Masetti N., D’Abrusco R., et al. (2014). Optical spectroscopic observations of blazars and γ -ray blazar candidates in the Sloan digital sky survey data release nine. The Astrophysical Journal, 148, 66. doi:10.1088/0004-6256/148/4/66

- [7] Laurent-Muehleisen S. A., Kollgaard R. I., Feigelson E. D., Brinkmann W., Siebert, J. (1999) The RGB Sample of Intermediate BL Lacertae Objects. *The Astrophysical Journal*, Volume 525, Issue 1, pp. 127-143.
- [8] Angioni R., Bissaldi E., Garrappa S., Longo F., Kocevski D. (2020) Fermi-LAT detection of a hard-spectrum GeV flare from the BL Lac B2 1811+31. *The Astronomer's Telegram*, No. 14060.
- [9] Angioni R. (2021) Fermi-LAT detection of gamma-ray flaring activity from the BL Lac GB6 J1058+2817. *The Astronomer's Telegram*, No. 14491.
- [10] Aleksić, J., Ansoldi, S., Antonelli, L. A., et al. 2016, *Astroparticle Physics*, 72, 76. doi:10.1016/j.astropartphys.2015.02.005
- [11] Blanch O. (2020) Detection of very-high-energy gamma-ray emission from B2 1811+31 with the MAGIC telescopes. *The Astronomer's Telegram*, No. 14090.
- [12] Blanch O. (2020) Detection of very-high-energy gamma-ray emission from GB6 J1058+2817 with the MAGIC telescopes. *The Astronomer's Telegram*, No. 14506.
- [13] R. Zanin et al. (2013) MARS, The MAGIC Analysis and Reconstruction Software. *Proceedings, 33rd International Cosmic Ray Conference (ICRC2013)*: Rio de Janeiro, Brazil, July 2-9.
- [14] Li and Y. Ma (1983) Analysis methods for results in gamma-ray astronomy. *Astrophysical Journal*, 272:317-324.
- [15] J. Albert et al. (2007) Unfolding of differential energy spectra in the MAGIC experiment. *Nuclear Instruments and Methods in Physics Research Section A*, Volume 583, Issue 2-3:494-506.
- [16] A. Domínguez et al. (2011) Extragalactic background light inferred from AEGIS galaxy-SED-type fractions. *MNRAS*, 410-4, 2556–2578.
- [17] Atwood W. B., Abdo A. A., Ackermann M. et al. (2009) The Large Area Telescope on the Fermi Gamma-Ray Space Telescope Mission. *The Astrophysical Journal*, Volume 697, Issue 2, pp. 1071-1102.

Full Authors List: MAGIC Collaboration

H. Abe¹, S. Abe¹, J. Abhir², V. A. Acciari³, I. Agudo⁴, T. Aniello⁵, S. Ansoldi^{6,46}, L. A. Antonelli⁵, A. Arbet Engels⁷, C. Arcaro⁸, M. Artero⁹, K. Asano¹, D. Baack¹⁰, A. Babić¹¹, A. Baquero¹², U. Barres de Almeida¹³, J. A. Barrio¹², I. Batković⁸, J. Baxter¹, J. Becerra González³, W. Bednarek¹⁴, E. Bernardini⁸, M. Bernardos⁴, J. Bernete¹⁵, A. Berti⁷, J. Besenrieder⁷, C. Bigongiari⁵, A. Biland², O. Blanch⁹, G. Bonnoli⁵, Ž. Bošnjak¹¹, I. Burelli⁶, G. Busetto⁸, A. Campoy-Ordaz¹⁶, A. Carosi⁵, R. Carosi¹⁷, M. Carretero-Castrillo¹⁸, A. J. Castro-Tirado⁴, D. Cerasole²³, G. Ceribella⁷, Y. Chai⁷, A. Chilingarian¹⁹, A. Cifuentes¹⁵, S. Cikota¹¹, E. Colombo³, J. L. Contreras¹², J. Cortina¹⁵, S. Covino⁵, G. D'Amico²⁰, V. D'Elia⁵, P. Da Vela^{17,47}, F. Dazzi⁵, A. De Angelis⁸, B. De Lotto⁶, A. Del Popolo²¹, M. Delfino^{9,48}, J. Delgado^{9,48}, C. Delgado Mendez¹⁵, D. Depaoli²², F. Di Pierro²², L. Di Venere²³, D. Dominis Preste²⁴, A. Donini⁵, D. Dorner²⁵, M. Doro⁸, D. Elsaesser¹⁰, G. Emery²⁶, J. Escudero⁴, L. Fariña⁹, A. Fattorini¹⁰, L. Foffano⁵, L. Font¹⁶, S. Fröse¹⁰, S. Fukami², Y. Fukazawa²⁷, R. J. García López³, M. Garczarczyk²⁸, S. Gasparyan²⁹, M. Gaug¹⁶, J. G. Giesbrecht Paiva¹³, N. Giglietto²³, F. Giordano²³, P. Gliwny¹⁴, N. Godinović³⁰, R. Grau⁹, D. Green⁷, J. G. Green⁷, D. Hadasch¹, A. Hahn⁷, T. Hassan¹⁵, L. Heckmann^{7,49}, J. Herrera³, D. Hrupec³¹, M. Hütten¹, R. Imazawa²⁷, T. Inada¹, R. Iotov²⁵, K. Ishio¹⁴, I. Jiménez Martínez¹⁵, J. Jormanainen³², D. Kerszberg⁹, G. W. Kluge^{20,50}, Y. Kobayashi¹, P. M. Kouch³², H. Kubo¹, J. Kushida³³, M. Láinez Lezáun¹², A. Lamastra⁵, D. Lelas³⁰, F. Leone⁵, E. Lindfors³², L. Linhof¹⁰, S. Lombardi⁵, F. Longo^{6,51}, R. López-Coto⁴, M. López-Moya¹², A. López-Oramas³, S. Loporchio²³, A. Lorini³⁴, E. Lyard²⁶, B. Machado de Oliveira Fraga¹³, P. Majumdar³⁵, M. Makariev³⁶, G. Maneva³⁶, N. Mang¹⁰, M. Manganaro²⁴, S. Mangano¹⁵, K. Mannheim²⁵, M. Mariotti⁸, M. Martínez⁹, M. Martínez-Chicharro¹⁵, A. Mas-Aguilar¹², D. Mazin^{1,52}, S. Menchiari³⁴, S. Mender¹⁰, S. Mićanović²⁴, D. Miceli⁸, T. Miener¹², J. M. Miranda³⁴, R. Mirzoyan⁷, M. Molero González³, E. Molina³, H. A. Mondal³⁵, A. Moralejo⁹, D. Morcuende¹², T. Nakamori³⁷, C. Nanci⁵, L. Nava⁵, V. Neustroev³⁸, L. Nickel¹⁰, M. Nievas Rosillo³, C. Nigro⁹, L. Nikolić³⁴, K. Nilsson³², K. Nishijima³³, T. Njoh Ekoume³, K. Noda³⁹, S. Nozaki⁷, Y. Ohtani¹, T. Oka⁴⁰, A. Okumura⁴¹, J. Otero-Santos³, S. Paiano⁵, M. Palatiello⁶, D. Paneque⁷, R. Paoletti³⁴, J. M. Paredes¹⁸, L. Pavletić²⁴, D. Pavlović²⁴, M. Persic^{6,53}, M. Pihet⁸, G. Pirola⁷, F. Podobnik³⁴, P. G. Prada Moroni¹⁷, E. Prandini⁸, G. Principe⁶, C. Priyadarshi⁹, W. Rhode¹⁰, M. Ribó¹⁸, J. Rico⁹, C. Righi⁵, N. Sahakyan²⁹, T. Saito¹, S. Sakurai¹, K. Satalecka³², F. G. Saturni⁵, B. Schleicher²⁵, K. Schmidt¹⁰, F. Schmuckermaier⁷, J. L. Schubert¹⁰, T. Schweizer⁷, A. Sciacaluga⁵, J. Sitarek¹⁴, V. Sliusar²⁶, D. Sobczynska¹⁴, A. Spolon⁸, A. Stamerra⁵, J. Striškov³¹, D. Strom⁷, M. Strzys¹, Y. Suda²⁷, T. Suric⁴², S. Suutarinen³², H. Tajima⁴¹, M. Takahashi⁴¹, R. Takeishi¹, F. Tavecchio⁵, P. Temnikov³⁶, K. Terauchi⁴⁰, T. Terzić²⁴, M. Teshima^{7,54}, L. Tosti⁴³, S. Truzzi³⁴, A. Tutone⁵, S. Ubach¹⁶, J. van Scherpenberg⁷, M. Vazquez Acosta³, S. Ventura³⁴, V. Verguillov³⁶, I. Viale⁸, C. F. Vigorito²², V. Vitale⁴⁴, I. Vovk¹, R. Walter²⁶, M. Will⁷, C. Wunderlich³⁴, T. Yamamoto⁴⁵, ¹ Japanese MAGIC Group: Institute for Cosmic Ray Research (ICRR), The University of Tokyo, Kashiwa, 277-8582 Chiba, Japan

² ETH Zürich, CH-8093 Zürich, Switzerland

³ Instituto de Astrofísica de Canarias and Dpto. de Astrofísica, Universidad de La Laguna, E-38200, La Laguna, Tenerife, Spain

⁴ Instituto de Astrofísica de Andalucía-CSIC, Glorieta de la Astronomía s/n, 18008, Granada, Spain

⁵ National Institute for Astrophysics (INAF), I-00136 Rome, Italy

⁶ Università di Udine and INFN Trieste, I-33100 Udine, Italy

⁷ Max-Planck-Institut für Physik, D-80805 München, Germany

⁸ Università di Padova and INFN, I-35131 Padova, Italy

⁹ Institut de Física d'Altes Energies (IFAE), The Barcelona Institute of Science and Technology (BIST), E-08193 Bellaterra (Barcelona), Spain

¹⁰ Technische Universität Dortmund, D-44221 Dortmund, Germany

¹¹ Croatian MAGIC Group: University of Zagreb, Faculty of Electrical Engineering and Computing (FER), 10000 Zagreb, Croatia

¹² IPARCOS Institute and EMFTel Department, Universidad Complutense de Madrid, E-28040 Madrid, Spain

¹³ Centro Brasileiro de Pesquisas Físicas (CBPF), 22290-180 URCA, Rio de Janeiro (RJ), Brazil

¹⁴ University of Lodz, Faculty of Physics and Applied Informatics, Department of Astrophysics, 90-236 Lodz, Poland

¹⁵ Centro de Investigaciones Energéticas, Medioambientales y Tecnológicas, E-28040 Madrid, Spain

¹⁶ Departament de Física, and CERES-IEEC, Universitat Autònoma de Barcelona, E-08193 Bellaterra, Spain

¹⁷ Università di Pisa and INFN Pisa, I-56126 Pisa, Italy

¹⁸ Universitat de Barcelona, ICCUB, IEEC-UB, E-08028 Barcelona, Spain

¹⁹ Armenian MAGIC Group: A. Alikhanyan National Science Laboratory, 0036 Yerevan, Armenia

²⁰ Department for Physics and Technology, University of Bergen, Norway

²¹ INFN MAGIC Group: INFN Sezione di Catania and Dipartimento di Fisica e Astronomia, University of Catania, I-95123 Catania, Italy

²² INFN MAGIC Group: INFN Sezione di Torino and Università degli Studi di Torino, I-10125 Torino, Italy

²³ INFN MAGIC Group: INFN Sezione di Bari and Dipartimento Interateneo di Fisica dell'Università e del Politecnico di Bari, I-70125 Bari, Italy

²⁴ Croatian MAGIC Group: University of Rijeka, Faculty of Physics, 51000 Rijeka, Croatia

²⁵ Universität Würzburg, D-97074 Würzburg, Germany

²⁶ University of Geneva, Chemin d'Ecogia 16, CH-1290 Versoix, Switzerland

²⁷ Japanese MAGIC Group: Physics Program, Graduate School of Advanced Science and Engineering, Hiroshima University, 739-8526 Hiroshima, Japan

²⁸ Deutsches Elektronen-Synchrotron (DESY), D-15738 Zeuthen, Germany

²⁹ Armenian MAGIC Group: ICRANet-Armenia, 0019 Yerevan, Armenia

- ³⁰ Croatian MAGIC Group: University of Split, Faculty of Electrical Engineering, Mechanical Engineering and Naval Architecture (FESB), 21000 Split, Croatia
- ³¹ Croatian MAGIC Group: Josip Juraj Strossmayer University of Osijek, Department of Physics, 31000 Osijek, Croatia
- ³² Finnish MAGIC Group: Finnish Centre for Astronomy with ESO, University of Turku, FI-20014 Turku, Finland
- ³³ Japanese MAGIC Group: Department of Physics, Tokai University, Hiratsuka, 259-1292 Kanagawa, Japan
- ³⁴ Università di Siena and INFN Pisa, I-53100 Siena, Italy
- ³⁵ Saha Institute of Nuclear Physics, A CI of Homi Bhabha National Institute, Kolkata 700064, West Bengal, India
- ³⁶ Inst. for Nucl. Research and Nucl. Energy, Bulgarian Academy of Sciences, BG-1784 Sofia, Bulgaria
- ³⁷ Japanese MAGIC Group: Department of Physics, Yamagata University, Yamagata 990-8560, Japan
- ³⁸ Finnish MAGIC Group: Space Physics and Astronomy Research Unit, University of Oulu, FI-90014 Oulu, Finland
- ³⁹ Japanese MAGIC Group: Chiba University, ICEHAP, 263-8522 Chiba, Japan
- ⁴⁰ Japanese MAGIC Group: Department of Physics, Kyoto University, 606-8502 Kyoto, Japan
- ⁴¹ Japanese MAGIC Group: Institute for Space-Earth Environmental Research and Kobayashi-Maskawa Institute for the Origin of Particles and the Universe, Nagoya University, 464-6801 Nagoya, Japan
- ⁴² Croatian MAGIC Group: Ruder Bošković Institute, 10000 Zagreb, Croatia
- ⁴³ INFN MAGIC Group: INFN Sezione di Perugia, I-06123 Perugia, Italy
- ⁴⁴ INFN MAGIC Group: INFN Roma Tor Vergata, I-00133 Roma, Italy
- ⁴⁵ Japanese MAGIC Group: Department of Physics, Konan University, Kobe, Hyogo 658-8501, Japan
- ⁴⁶ also at International Center for Relativistic Astrophysics (ICRA), Rome, Italy
- ⁴⁷ now at Institute for Astro- and Particle Physics, University of Innsbruck, A-6020 Innsbruck, Austria
- ⁴⁸ also at Port d'Informació Científica (PIC), E-08193 Bellaterra (Barcelona), Spain
- ⁴⁹ also at Institute for Astro- and Particle Physics, University of Innsbruck, A-6020 Innsbruck, Austria
- ⁵⁰ also at Department of Physics, University of Oslo, Norway
- ⁵¹ also at Dipartimento di Fisica, Università di Trieste, I-34127 Trieste, Italy
- ⁵² Max-Planck-Institut für Physik, D-80805 München, Germany
- ⁵³ also at INAF Padova
- ⁵⁴ Japanese MAGIC Group: Institute for Cosmic Ray Research (ICRR), The University of Tokyo, Kashiwa, 277-8582 Chiba, Japan